A 3D-printed broadband millimeter wave absorber

Matthew Petroff [1] John Appel [1] Karwan Rostem [2] Charles L. Bennett [1] Joseph Eimer [1] Tobias Marriage [1] Joshua Ramirez [3] Edward J. Wollack [2]

[1]Johns Hopkins University [2]NASA Goddard Space Flight Center [3]Johns Hopkins Applied Physics Laboratory

arXiv: 1808.00820

Introduction

The ongoing development of increasingly sensitive cosmic microwave background (CMB) telescopes requires commensurate improvements in the control of systematic errors. One such source of error is from stray light, which needs to be controlled through the use of millimeter wave absorbers, both under ambient conditions and within cryogenic receivers [1]. Since the field is moving towards the use of multichroic detectors with wide frequency bands in a shared optical path [2], broadband absorbers are required. Per this application, the frequency range from 30 GHz to 230 GHz is of interest, since it covers the CMB emission peak as well as synchrotron and thermal dust foregrounds.

In recent years, additive manufacturing in the form of 3D printing has become increasingly common, in particular fused filament fabrication (FFF). FFF-based printing works by extruding a plastic filament through a heated nozzle mounted on a CNC stage, which builds up objects layer-by-layer [3]. This allows for rapid prototyping and for manufacturing easily customized designs and one-off parts.

Graded index absorbers generally take the form of an array of pyramidal structures. While a periodic pyramidal structure makes for an effective absorber, it is not well suited for FFF-based printing. When sliced into layers for FFF-based printing, each pyramid slice is disconnected from the others in a given layer. Thus, the filament extrusion process must be stopped and the filament retracted for each and every pyramid slice, which prevents the creation of sharp points. Furthermore, prints are usually weakest along layer lines, making points liable to break off. To avoid these issues, a geometric approximation of a space-filling curve is used, which fills the plane with a continuous wedge.

Space-filling curves

A space-filling curve is a curve that passes through every point of a two-dimensional area [4]. This type of mathematical monster was first described by Peano [5]. Shortly thereafter, Hilbert described another such curve but also described an iterative sequence of geometric approximations to his curve [6]. Importantly, this type of geometric approximation can be physically realized.

Space-filling curves are self-similar [4]. Thus, absorbers created from different order geometric approximations of space-fillings curves, in this work the square-filling Hilbert curve, will exhibit similar behavior. Although a Hilbert curve has only 1-fold symmetry, geometric approximations of the Hilbert curve have asymptotically equal numbers of uniformly distributed horizontal and vertical line segments [7]; thus, they should not show a net polarization response in reflectivity, unlike 2-fold symmetric absorbers created from sets of parallel wedges.

To create an absorber, a wedge was modeled such that the peak of the wedge follows the centerline of a geometric approximation of the Hilbert curve. The wedge then extends down such that the halfway point between segments of the curve form troughs. Furthermore, only a shell is printed, leaving the inside hollow, to reduce printing time and save on material use.

Material selection

Two different material candidates were tested, a commercially available carbon-loaded conductive PLA filament and a high impact polystyrene (HIPS) filament custom extruded from a commercially available carbon-loaded conductive HIPS pellet. The complex relative dielectric functions of the candidate materials as well as plain PLA and plain HIPS plastics were characterized using a pair of filled rectangular waveguide sections for each material. Using a modeling approach described in existing literature [8], the dielectric functions were extracted from scattering parameters measured from 22 GHz to 40 GHz using a vector network analyzer (VNA).

Material	ϵ_r'	ϵ_r''
Avantra 8130 HIPS	2.49	0.003
Ingeo 4043D PLA	2.80	0.03
PS-715 Carbon-loaded HIPS	7.7	2.1
Proto-pasta Conductive PLA	15.0	15.0

Table 1: Dielectric function measurement results for bulk plastic samples in waveguide section fixtures are presented. The observed relative error of the dielectric function for the average of each set of samples is < 0.01 for the real component, ϵ_r', and < 0.12 for the imaginary component, ϵ_r''.

Of the materials tested, the carbon-loaded HIPS is the best candidate for an absorber, since it is an absorptive dielectric that is not too reflective. The carbon-loaded PLA is much more conductive and behaves like a poor metal, making it too reflective for this application. Without carbon loading, the HIPS is a low-loss dielectric, while the PLA is a nylon-like, relatively lossy dielectric.

Electromagnetic modeling

A small unit cell of the absorber was modeled in the ANSYS HFSS software package, which performs an electromagnetic finite element analysis (FEA), using periodic boundary conditions. A second order Hilbert curve was used as a unit cell for the absorber, since it has greater symmetry than a first order curve—and thus lower residual polarization response—while having reduced simulation complexity when compared to higher order curves. Reflectivity at normal incidence was simulated.

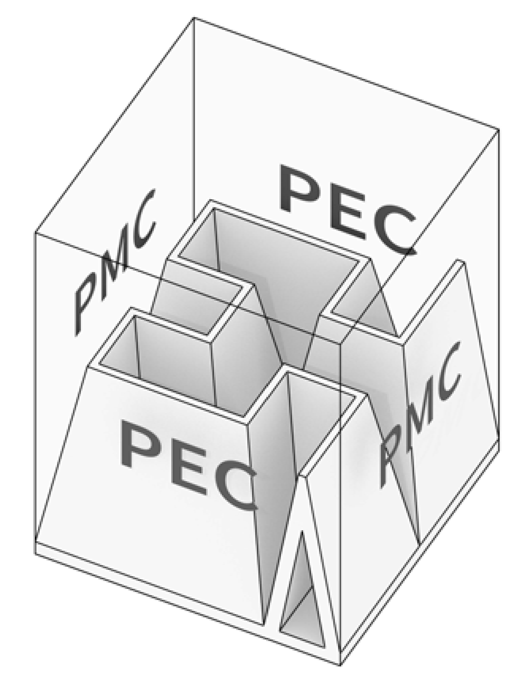

Figure 1: The unit cell used in simulations, a second order Hilbert curve, is shown. Periodic boundary conditions were established by using perfect electric conductors (PECs) for the front and back faces of the bounding prism and perfect magnetic conductors (PMCs) for the left and right faces of the bounding prism. The top face of the prism was used as a wave port, and the bottom face was set as a PEC.

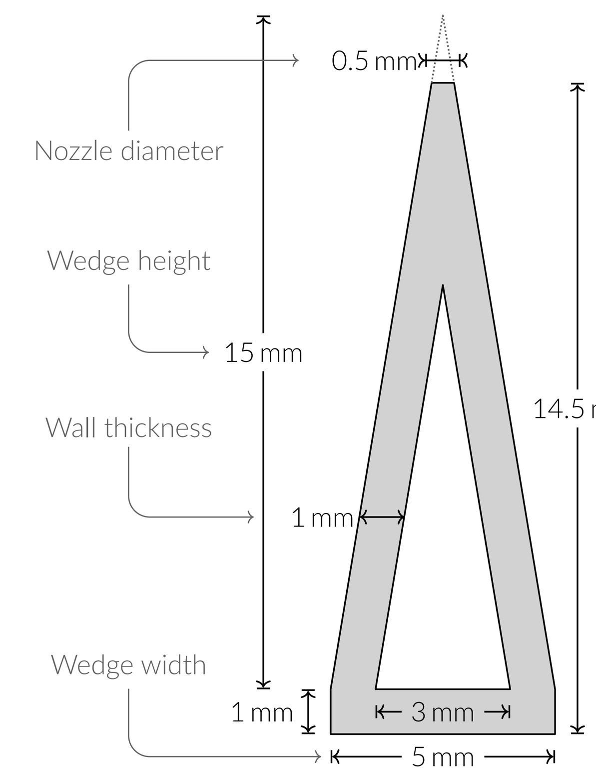

Figure 2: A cross section of the absorber wedge is shown, labeled with the dimensions used for the measured prototype, which utilizes a double wall printed with a 0.5 mm nozzle. Due to the nozzle diameter, the wedge tip is truncated.

Different wall thicknesses, including a solid cross section, were simulated for the conductive HIPS, as were orthogonal polarizations. Additionally, the conductive HIPS was simulated with varying degrees of conductivity. Possible wall thicknesses are quantized by the diameter of the 3D printer's extrusion nozzle, 0.5 mm in this case. Unless otherwise noted, a double nozzle diameter wall thickness, with a thickness of 1 mm and manufactured with two parallel passes of the printer's extrusion nozzle, and a 3:1 wedge height to wedge width aspect ratio was used (before truncation due to nozzle diameter). A 2:1 aspect ratio was also tried. To simulate orthogonal polarization, the PEC and PMC boundaries were switched.

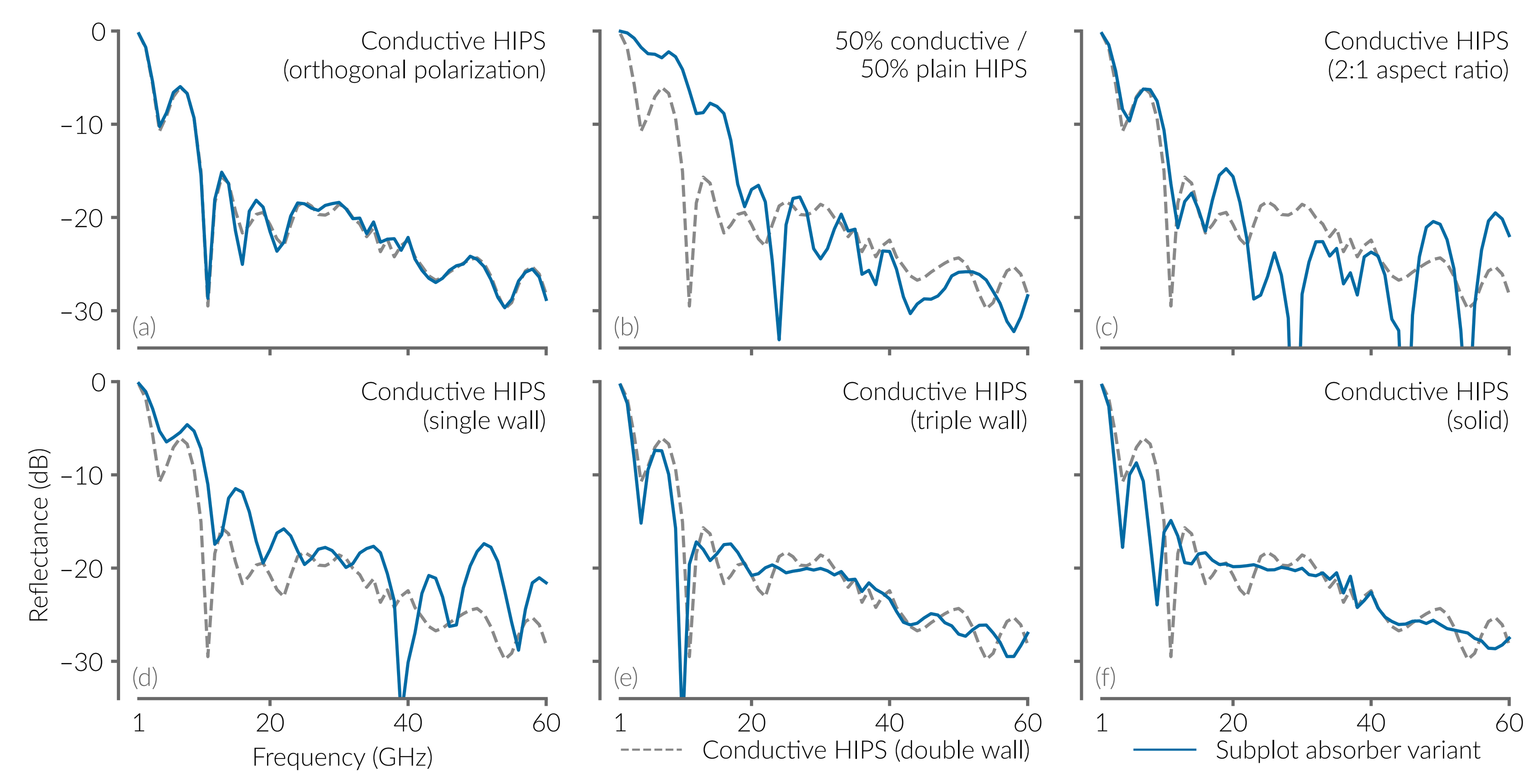

Figure 3: The results of FEA reflection simulations of absorber variants (solid) are shown against the baseline simulation of a carbon-loaded HIPS absorber with the geometry shown in Figure 2 (dashed). Each simulation was performed from 1 GHz to 60 GHz at an interval of 1 GHz. The reflectance is shown as a function of frequency for six absorber variants.

The simulation data show good polarization symmetry, which supports the unit cell choice. The equal mix of carbon-loaded HIPS and plain HIPS shows slightly better performance than the carbon-loaded HIPS alone, but it was decided that this marginal improvement was not worth the extra effort in filament manufacturing, so a mix was not used for prototyping. The triple wall and solid cross section simulation results were quite similar to the double wall simulation results, so the double wall was used, as this reduces printing time and material usage without negatively affecting the reflectivity.

Fabrication

Using a script utilizing a solid modeling scripting library and specific design parameters, a solid model for an absorber was procedurally generated and then converted to G-code instructions for the 3D printer were generated using slicer software. The absorber prototype was then printed on a LulzBot TAZ 6 FFF 3D printer out of carbon-loaded HIPS. It is a fifth order Hilbert curve with a square footprint of 160 mm by 160 mm, a total height of 14.5 mm, a double wall, and 3:1 aspect ratio.

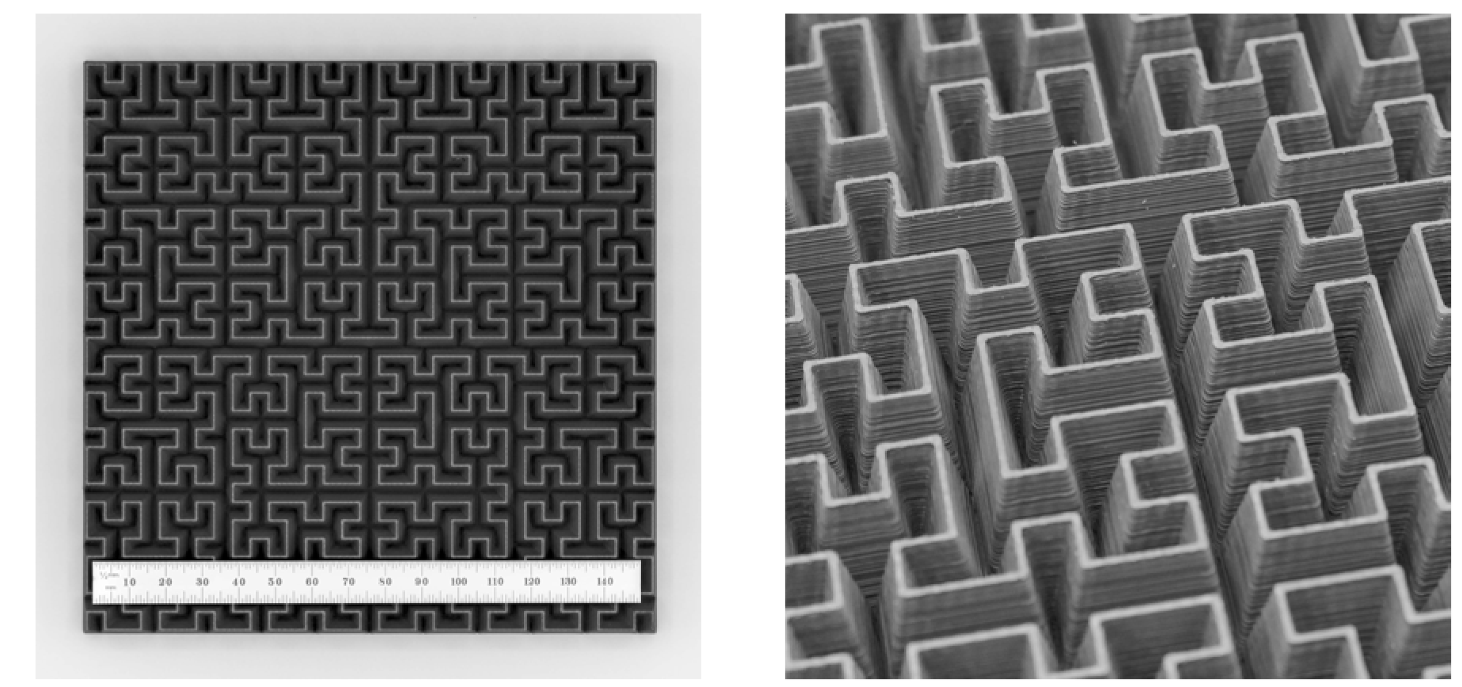

Figure 4: The prototype carbon-loaded HIPS Hilbert curve is shown. The left picture shows the full 160 mm square absorber, while the right picture shows a detailed view in which layer lines from the 3D printing process are visible.

Measurement

The fabricated absorber prototype was measured in two waveguide bands using a VNA coupled to a free space quasi-optical setup [9]; there is good agreement between the measurements and electromagnetic simulations. Furthermore, prototypes have been successfully used cryogenically at 60 K for stray light absorption, surviving dozens of thermal cycles, and have been successfully cooled using liquid nitrogen for use as cold loads.

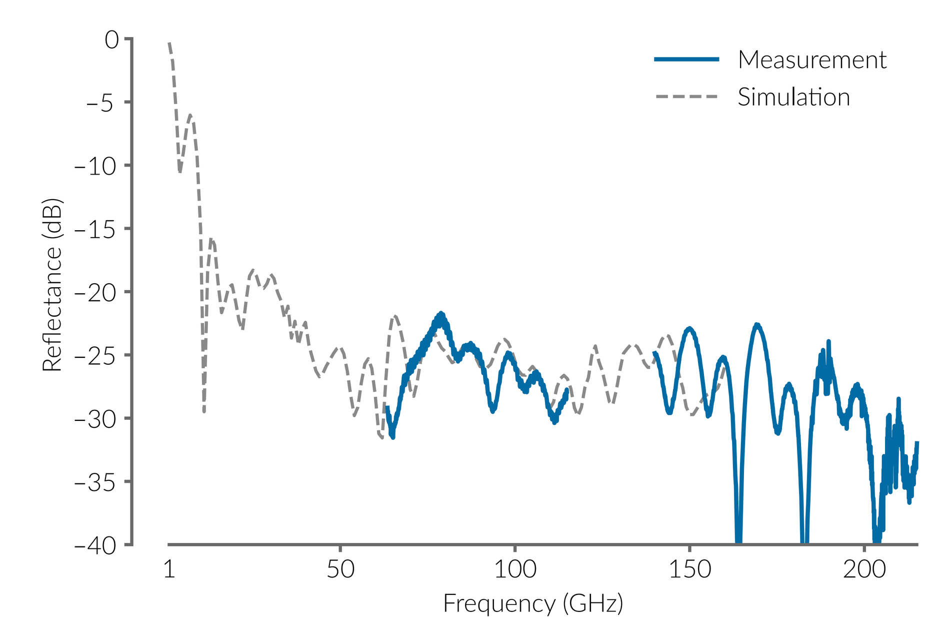

Figure 5: Reflectance measurement results (solid) are shown along with values predicted by simulation (dashed).

Acknowledgments & References

This work was supported by a Space@Hopkins seed grant. J. Appel, C. Bennett, J. Eimer, T. Marriage, and M. Petroff are supported via National Science Foundation Division of Astronomical Sciences grants for the Cosmology Large Angular Scale Surveyor (CLASS), grant numbers 0959349, 1429236, 1636634, and 1654494.

[1] K. Harrington et al. "The Cosmology Large Angular Scale Surveyor". In: *Millimeter, Submillimeter, and Far-Infrared Detectors and Instrumentation for Astronomy VIII*. Vol. 9914. Proc. SPIE. July 2016, 99141K. DOI: 10.1117/12.2233125. arXiv: 1608.08234 [astro-ph.IM].

[2] M. H. Abitbol et al. "CMB-S4 Technology Book, First Edition". In: *ArXiv e-prints* (June 2017). arXiv: 1706.02464 [astro-ph.IM].

[3] Rhys Jones et al. "RepRap — the replicating rapid prototyper". In: *Robotica* 29.1 (2011), pp. 177–191. DOI: 10.1017/S026357471000069X.

[4] Hans Sagan. *Space-Filling Curves*. New York: Springer-Verlag, 1994. ISBN: 0387942653.

[5] Giuseppe Peano. "Sur une courbe, qui remplit toute une aire plane". In: *Math. Ann.* 36.1 (Mar. 1890), pp. 157–160. ISSN: 1432-1807. DOI: 10.1007/BF01199438.

[6] David Hilbert. "Ueber die stetige Abbildung einer Linie auf ein Flächenstück". In: *Math. Ann.* 38.3 (1891), pp. 459–460. ISSN: 1432-1807. DOI: 10.1007/BF01199431.

[7] B. Moon et al. "Analysis of the clustering properties of the Hilbert space-filling curve". In: *IEEE Trans. Knowl. Data Eng.* 13.1 (Jan. 2001), pp. 124–141. ISSN: 1041-4347. DOI: 10.1109/69.908985.

[8] E. J. Wollack et al. "Electromagnetic and Thermal Properties of a Conductively Loaded Epoxy". In: *Int. J. Infrared Millimeter Waves* 29.1 (2008), pp. 51–61. ISSN: 1572-9559. DOI: 10.1007/s10762-007-9299-4.

[9] David T. Chuss et al. "A cryogenic thermal source for detector array characterization". In: *Rev. Sci. Instrum.* 88.10 (2017), p. 104501. ISSN: 1089-7623. DOI: 10.1063/1.4996751. arXiv: 1707.05879 [astro-ph.IM].